ELSEVIER

Turbulent structure of an axisymmetric plume penetrating a strong density stratification

L. Dehmani,* Doan Kim-Son, and L. Gbahoué
Laboratoire d'Etudes Thermiques de l'Ecole Nationale Supérieure de Mécanique et d'Aérotechnique, Futuroscope Cedex, France

The interaction between a turbulent plume and a strong stratified layer is studied for three experimental configurations with different buoyancy and ambient stratification. The investigation of the turbulent structure of these axisymmetric flows was first carried out under ambient conditions of high constant density at the origin of the flow. The interaction with a stratified environment was then analyzed. The difficulty in penetrating the stratified media was due to a large expansion of the flow and a change of the direction of the radial velocity close to the axis. A decrease of the kinetic turbulent energy was observed at the crossing of the neutral zone.

Keywords: axisymmetric plume; density stratification; turbulent structure

Introduction

The discharge of a buoyant plume into a stratified environment is a phenomenon which often occurs in natural and in industrial surroundings. Lakes, rivers, and ponds are frequently stably stratified, with the density increasing with the depth.

At the early stages of fire growth in an enclosed region, the heat input due to the fire generally results in the establishment of a hot upper layer with low density above a cooler and heavier bottom layer. Owing to the buoyancy, the density within each layer is fairly uniform. Very often, a sharp interface is created between the two media. At this interface, the density gradient corresponding to a strong stratification is very high and strongly affects the turbulence characteristics of the flow. Unlike pure jets, the development of plumes in stratified media has rarely been investigated.

Jaluria and Himasekhar (1983) carried out a numerical study of a two-dimensional (2-D) thermal plume evolving in a thermally stratified environment. The stratification was characterized by an additional term appearing in the energy equation. The presence of stratification decreases the buoyancy level in the flow, which leads to a decrease in the centreline velocity and eventually to a zero velocity, followed in turn by a possible flow reversal.

Srinivasan and Angirasa (1990) made a numerical study of an axisymmetric plume. However, they only analyzed through an increase with height of a linear temperature the case of a laminar flow evolving in a stratified medium. In this case, they analyzed the interaction between the buoyancy ratio, the thermal stratification, and the Prandtl and Schmidt numbers.

Other authors investigated two-layer models in which the stratified medium was divided into two layers: a lower cold layer and an upper hot layer. They presumed that the transfer of heat and of mass between these two layers was made only by the plume. Basing his investigation on this hypothesis, Evans (1983) developed methods for determining the axial gas flow conditions inside a weakly buoyant plume. Cooper (1983) modeled flow conditions depending on the density difference between the two layers on the strength of the source and its position below the interface. Finally, Kapoor and Jaluria (1993) studied the penetrative characteristics of a heated 2-D, turbulent wall jet discharged downward into a two-layer thermally stable environment.

It can be seen from this brief review that previous investigations have generally been limited to the overall analysis of weakly buoyant flows impinging a weak ambient stratification. Information concerning the fine structure of turbulent plumes interacting with strong stratified media have not been extensively investigated, particularly as far as the correlation coefficients are concerned. However, this information is essential for carrying out a numerical such modelling as a $k-\varepsilon$ model.

In the present work, we are concerned with the characteristics of both the mean and the turbulent fields of the mass plume. The investigation includes the source area up to the level of a strong stratification. The plume development in a neutral environment is then studied. This investigation has been carried out for three configurations, corresponding to different experimental conditions in which the buoyancy in the flow and the stratification intensity have varied.

Experimental arrangement

The experimental arrangement was specially supported so as to obtain a plume with a very weak momentum at the source. The

*Present address: Faculté des Sciences de Tunis, Département de Physique, Campus Universitaire de Tunis (Tunisie)

Address reprint requests to Doan Kim-Son, Laboratoire d'Etudes Thermique de l'Ecole Nationale Supérieure de Mécanique et d'Aérotechnique, BP. 109, 86960 Futuroscope Cedex, France.

Received 9 August 1995; accepted 8 March 1996

Int. J. Heat and Fluid Flow 17: 452–459, 1996

655 Avenue of the Americas, New York, NY 10010

0142-727X/96/$15.00
PII S0142-727X(96)00050-3

flow was submitted to strong buoyancy forces and had to penetrate a stable stratified medium. The experimental realization of such a flow was very difficult to carry out, which was why a similarity investigation had been made previously. The flow could be simulated by an air–helium mixing axisymmetric jet with a weak initial density and a weak velocity at the source.

The inner-diameter of the nozzle tube used for the experiments was 0.053 m. This source was insulated by a large glass box of 2 m height, and a 1.20 m × 1.20 m square section. This configuration made is possible to obtain a quiet flow with regard to the surrounding perturbations.

The ambient stratification was carried out by putting a 0.3 m × 0.8 m × 0.8 m cavity at a height of about two diameters above the source. This cavity was open only at the bottom and fed by the flow composed by a mixture of the helium plume and the entrained air (Figure 1). The excess of mixture flowing out from the cavity was drained off without any further interaction with the incoming flow: a vent was made in the axis of the 5-mm thick glass casing by piercing a round hole with a 105-mm diameter. The effluent flowed out radially through a wire netting ring with a 260-mm diameter and a 55-mm height. This arrangement enabled the build up of a stable thin layer, with a high-density gradient between the ambient air and the neutral stratification of the helium–air mixing in the cavity, by diminishing the load loss.

The velocity components were simultaneously measured by laser-Doppler anemometry (LDA), the flow being seeded by a spray of submicronic oil particles. The errors on the velocity measurements due to particle drag were below 10% for velocities not exceeding 0.10 m/s and 1% for higher velocities. During the experiments, only the instruments of measurement are displaced. The source whose characteristics have already been described remain fixed during the tests, which has the advantage of not disturbing the flow. The LDA, with its optical system, and the photomultipliers are assembled on a displacement carriage equipped with micrometric step motors which can be tridimensionally monitored (x, y, z) with a minicomputer. The Doppler signals are processed by two burst spectrum analysers (BSA), one for each of the velocity components u, v. These are monitored by the minicomputer to which they are connected.

The concentrations were measured by an oxygen analyzer with a zirconium oxide sensor; this device allowed the measurement of oxygen concentrations varying from 100% down to

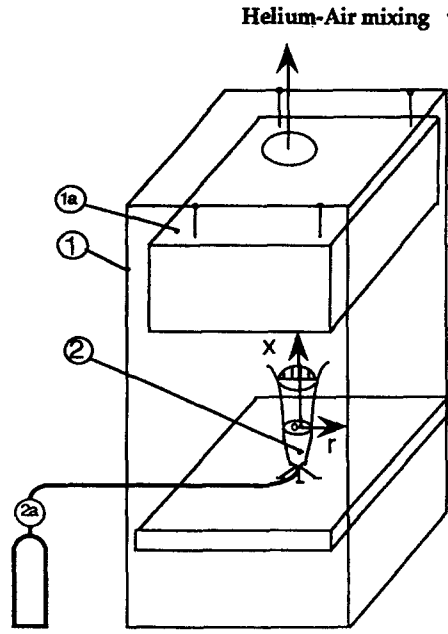

1 - Glass-sight cabin **2 - Nozzle-tube**
1a - Stratification cavity **2a - Helium reservoir**

Figure 1 Experimental setup

traces. This analyzer gave an electric signal which varied linearly with the oxygen content of the sample. From these values, the content of helium and the density of the sample were deduced.

Three experimental configurations designated as (A), (B), and (C) are shown in Table 1:

(1) Configuration (A) with a very strong buoyancy, like a pure plume, corresponding to the minimum helium flow rate determined by the experimental equipment

(2) For a better account of the influence of the force of inertia, configuration (C), with a strong momentum at the source corresponding to the maximum flow rate available, was also considered.

Notation

$d = 2r_0$	diameter of the source
Fr	Froude number (at the source $= u_0^2 \rho_{H_e} / g d(\rho_{\text{air}} - \rho_{H_e})$)
g	magnitude of gravitational acceleration
I	turbulence intensity
I_u	intensity of the turbulence of the axial velocity component
I_v	intensity of the turbulence of the radial velocity component
$\bar{k}$	mean turbulence kinetic energy
r	radial coordinate
r_1'	radial coordinate at the point where $\Delta\bar{\rho}/\overline{\rho_c} = 1/e$
Re	Reynolds number
Ri	Richardson number ($\text{Ri} = \text{Fr}^{-1/2}$)
N	BRUNT-VÄISÄLÄ frequency $\{N^2 = -(g/\rho_{\infty 0})(d\rho_{\infty 0}/dx)\}$
u	vertical velocity component
v	radial velocity component
x	vertical coordinate distance
$\hat{x} = x/d$	dimensionless vertical coordinate distance

Greek

ρ	fluid density
$\rho_{\infty 0}$	ambient fluid density at $x = 0$

Subscripts

c	on the axis of the flow
0	condition at the source
u	corresponding to the vertical velocity
v	corresponding to the radial velocity
∞	ambient conditions

Superscripts

$\wedge$	dimensionless value
$\bar{}$	mean value
$'$	fluctuation

Table 1 Characteristic dimensionless numbers

Configurations	$1000.Fr_0$	Re_0	$\rho_{\infty max}/\rho_{\infty min}$
(A)	1.16	27.31	0.93
(B)	10.54	82.43	0.81
(C)	63.12	201.71	0.64

(3) Finally, an intermediate configuration (B) with a strong contribution of buoyancy and inertia forces, completed the experimental program.

Three zones can then be observed. Close to the source, the *plume zone* with a weak density controlled by the initial conditions, flowed through a homogeneous ambient medium at the air density value. At about two diameters above the injector, the *neutral zone*, fed by a mixing of helium and entrained air in a proportion which varied with the configuration was investigated. The density within this zone was fairly uniform. These two zones, each with its specific uniform density, were separated by an *interaction zone*. In this interface, the turbulence characteristics of the flow were strongly modified by a steep linear density gradient. Within this zone, the stratification was stable and characterized by a BRUNT-VÄISÄLÄ frequency (N^2) that varied with the experimental conditions. It was equal to 10.89 s^{-2} for configuration (A) and 57.70 s^{-2} for configuration (C); the value for configuration (B) was $N^2 = 31.18\ s^{-2}$. Thus, the stratification coefficient seemed to increase when the Reynolds and Froude numbers at the source increased. The values of N^2 were two orders of magnitude greater than the standard values encountered in the literature, where N^2 is generally below 0.5 s^{-2}, as has been shown by Chen and Rodi (1980).

The dimensionless numbers characterizing the initial conditions of the flow as well as the ratio $\rho_{\infty max}/\rho_{\infty min}$ of the maximum to the minimum ambient density are shown in Table 1. This shows that the value at the source, Fr_0, is greater than the Fr_0 of flames with large buoyancy effects, but close to that of pure plumes (Table 2) especially with configuration (A), which has a very weak momentum at the source (low Re_0). Configuration (C) with the highest Re and Fr appears to be closer to those of a hot jet. The interaction between the turbulent plume and a strong stratified medium is developed in the following sections.

Results and discussion

The change of the mean density and mean velocity are investigated using the experimental conditions described, after which the dynamic fluctuations, particularly concerning the turbulence intensities and the distribution of the turbulence kinetic energy, are studied.

Mean density field

Figure 2 shows the radial variations of the mean density for the three configurations. The behavior of $\bar{\rho}$ changes with the flows.

Table 2 Froude number review

Authors	Nature of the flow	Fr_0
Vachon and Champion (1986)	Flame with large buoyancy effects	10^{-6}–10^{-4}
Guillou (1984)	Pure buoyant plume (heated portion of a sphere)	$3.45.10^{-4}$
Brahimi (1987)	Pure buoyant plume (heated disk)	2.10^{-4}
Gebhart et al. (1984)	Hot jets	1–4.10^{4}

In the plume zone that corresponds to the flow development, the profiles are symmetrical and regular ($\hat{x} \leq 1.25$). However, they are characterized by a strong change in form and amplitude. The density distribution is practically homogeneous at the source, assuming an upside down top hat shape, followed by a steep gradient on each side (Figure 2a); when the height increases, the profiles become bell-shaped giving a continuous transverse density gradient; a minimum density is located at the axis (Figure 2b). This gradient due to the strong air entrainment by the plume (see the Dynamic field section), increases with the momentum at the source and reaches very high values in the case of configuration (C).

At the beginning of the interface area, the profiles become very flat. This flattening of the flow increases when the initial flow rate is weak, so it becomes difficult for the flow to penetrate the upper layer. At the beginning of the neutral zone, the density is still exposed to very weak variations, then tends uniformly to the appropriate value of the density of the ambient. The flow is transformed into a pure jet which develops due only to the forces of inertia.

Dynamic field

The different changes of the density seen above influence the velocity variations. The mean and the fluctuating components of the dynamic field is now examined in order to understand better the change of the turbulent structure of the flow and its interaction with the stratification.

Mean velocities. The radial profiles of the mean vertical velocity for different dimensionless heights are shown in Figure 3. This figure represents the variations of $\bar{u}$ only for configuration (B), because the same change is observed for the two others. Intense variations are observed when we move from one flow area to the other.

Just at the outlet of the injector ($\hat{x} = 0.05$), the profile presents two small peaks close to the axis instead of on it. Then, when the dimensionless axial coordinate $\hat{x}$ increases, the radial distribution becomes more regular and Gaussian-wise. The flow is exposed to an acceleration which increases with the injection flow rate. This phenomenon is induced by the strong density difference between the flow and the ambient medium; here the buoyancy forces are predominant. This area, close to the source, represents the flow development stage, characterized by a significant change both of the shape and the amplitude of the velocity profiles, as has been remarked above for the density profiles. At the extremity of this zone, the velocity reaches its maximum value corresponding to the balance between the buoyancy forces and the forces of viscosity and turbulence.

Measurements at $\hat{x} = 2.06$ and $\hat{x} = 2.38$, reveal the existence of a strong stability zone round that area. The profiles become flatter, showing a large expansion of the flow and a strong decrease of the vertical velocity (measurements at $\hat{x} = 3.25$). The flattening noticed at the interface increases when the injection flow rate at the source is weak; in this case, the inertia forces do not allow a good penetration of the flow into the upper layer so that the flattening effect is very pronounced. In the neutral region, the flow rate diminishes, for configuration (A). This is very rapid, and the flow evolves only because of the forces of inertia.

Figure 4 shows the change of the mean radial velocity for configuration (B), the same variation being observed for the two other configurations. Apparently, owing to these results, the radial velocity is rather weak and rarely exceeds 0.10 m/s to become equal to zero at the flow axis in agreement with the flow symmetry.

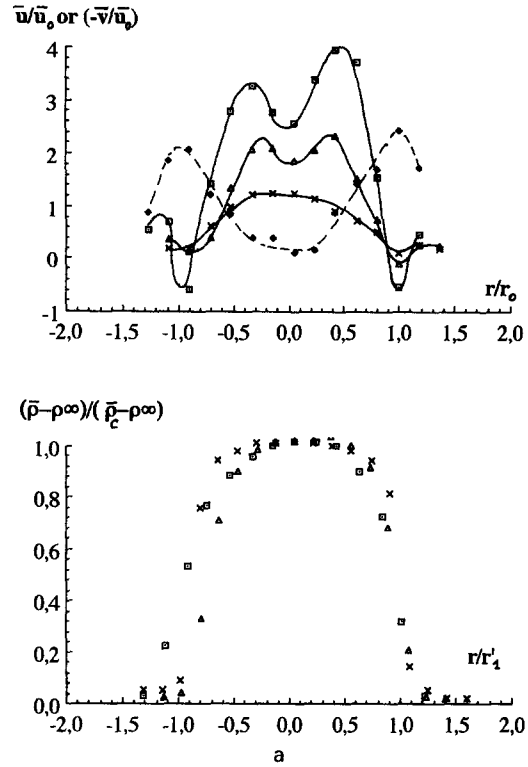

Figure 2a Radial distribution of the properties close to the nozzle. measurements are $x/d=0.05$; for $\bar{\rho}-\rho_\infty/\bar{\rho}_c-\rho_\infty$ or $\bar{u}/\bar{u}_0$: (□) (A), $\bar{u}_0=0.06$ m/s; (△) (B), $\bar{u}_0=0.19$ m/s; (×) (C), $\bar{u}_0=0.45$ m/s; for $(-\bar{v})/\bar{u}_0$: (◆) (A), $\bar{u}_0=0.06$ m/s

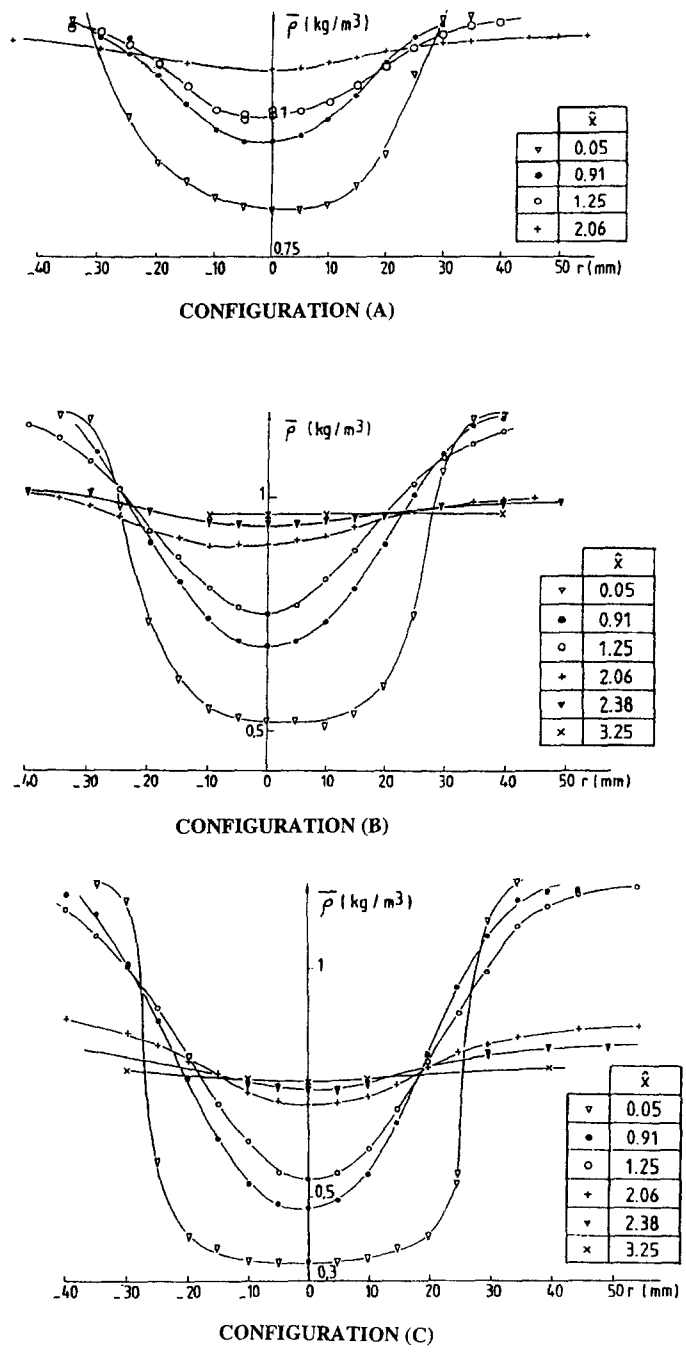

Figure 2b Radial distribution of the mean density

Near the injector, at $\hat{x}=0.05$, we can clearly discern two symmetrical extremes close to the edges of the injector. These are generated by the buoyancy forces which make the flow accelerate strongly thus resulting in a significant horizontal air entrainment.

From $\hat{x}=0.91$ onwards, the entrainment of the ambient air to the core of the plume becomes weaker. The zones with strong air entrainment move away from the flow axis when the height $\hat{x}$ increases. This phenomenon seems to be caused by the decrease of the density difference between the flow and the ambient.

At the interface close to $\hat{x}=2.06$, the plume flattens out and the radial velocity changes direction: close to the axis it is directed towards the outer part of the flow, and, when it moves away from the axis, it reaches its maximum, then decreases and changes direction. The radial velocity, therefore, becomes an "entrainment" velocity away from the plume core. This phenomenon could be related to the decrease of the vertical velocity near the axis, where the flow tends to flatten out when the height $\hat{x}$ increases. The horizontal velocity is directed towards the outer part of the flow. On the contrary, away from the core of the flow, the vertical velocity component $\bar{u}$ increases causing a suction of the ambient air and an "entrainment" velocity. Consequently, inside this very stable zone, an increase of the injection flow leads to higher values of the radial velocity $\bar{v}$ and a better symmetry of its profiles. Lastly, $\bar{v}$ grows weaker inside the neutral region, and the air entrainment is present only at the edges of the flow.

Turbulence intensities. Figure 5 shows that the turbulence intensity I_u behaves as a very slowly varying function near the core of the flow, when the altitude $\hat{x}$ increases. The profiles of configuration (A) show two roughly symmetrical maxima in the injector area; this is not at all the case with the other configurations. The presence of these two maxima values for the $\bar{u}$-intensity of turbulence was also noticed by Gengembre (1983) and Guillou (1984). It seems that this phenomenon is related to a more general mechanism, due to the motion of vortex structure in the core of the flow caused by the strong air entrainment. The profiles of I_u become flat, and the plume expands considerably, because of the impingement at the interface. Last, in the neutral zone, I_u can be roughly assumed to be uniform over a section of the flow (Figure 5).

On the axis of the flow, the mean value of the turbulence intensity is practically equal to 0.45 and varies very little from one configuration to another. Compared to the values found by Guillou et al. (1986) for a pure thermal plume, this value is as

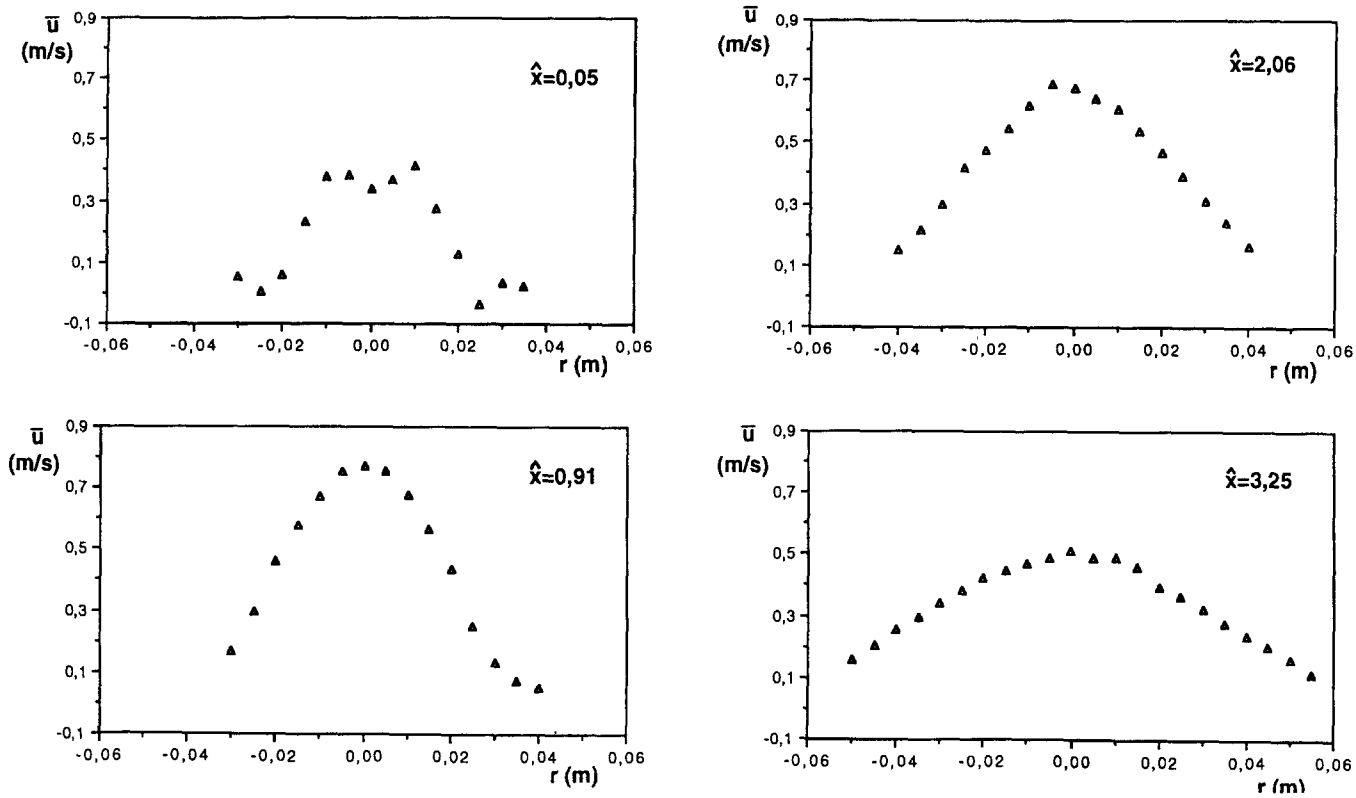

Figure 3 Radial distribution of the vertical mean velocity: Configuration (B)

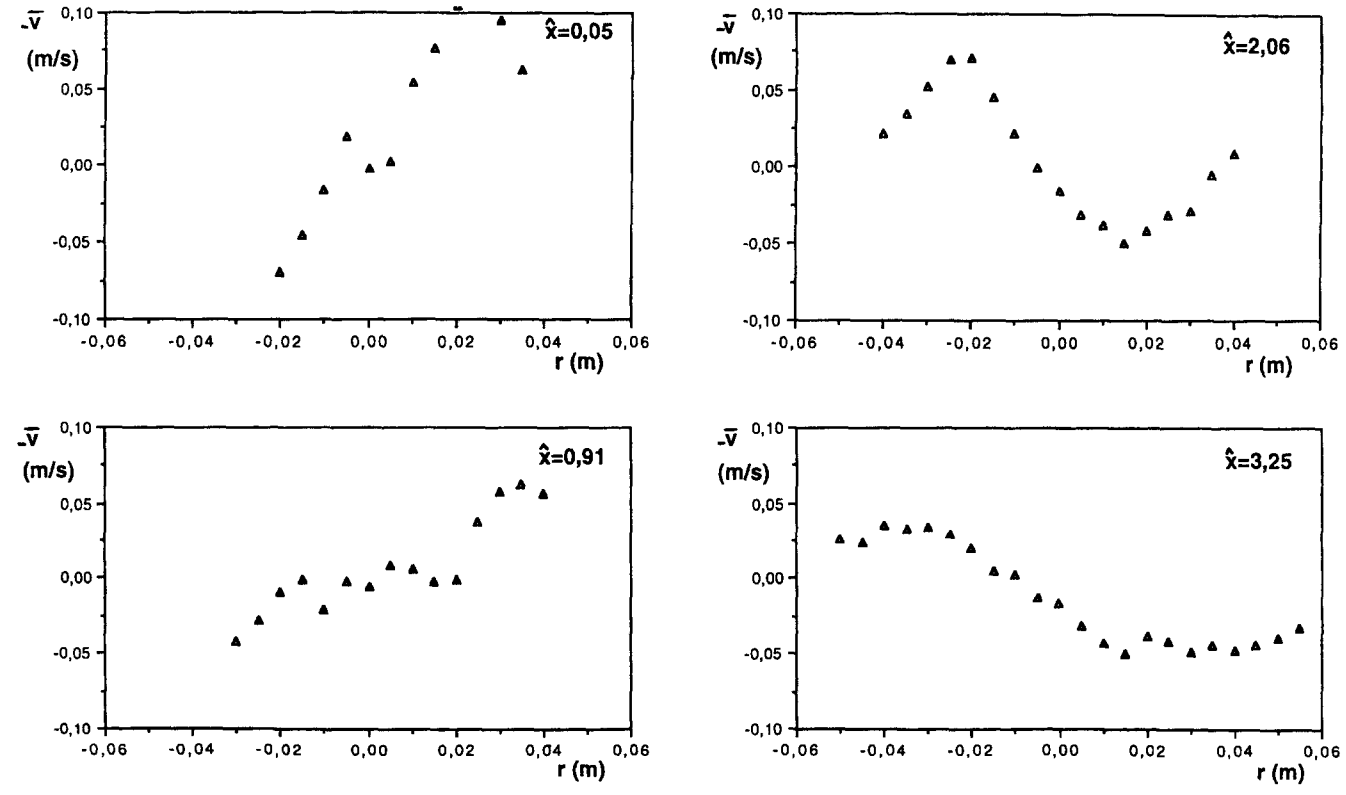

Figure 4 Radial distribution of the horizontal mean velocity: Configuration (B)

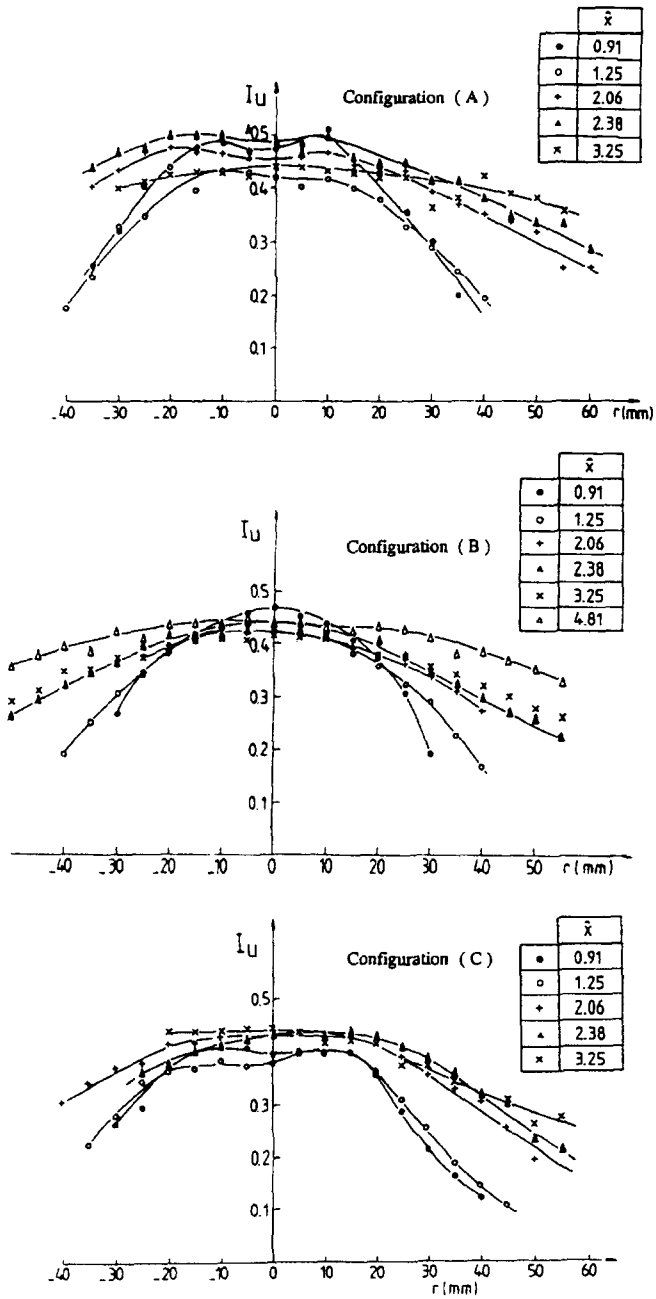

Figure 5 Turbulence intensity of the vertical velocity

high and in the same order (Table 3). This could be due to the strong entrainment which occurs in the case of a flow created by buoyancy forces.

As for the radial profiles of the turbulence intensity of the horizontal velocity fluctuations, they present a maximum at the core of the flow for whatever configuration is considered (Figure 6). For weak flow rates, (A); I_v experiences some difference in the growth between $\hat{x} = 0.91$ and $\hat{x} = 1.25$, contrary to the two other configurations in which the profiles are practically identical between these two heights. Inside this plume zone, the weakest intensity of turbulence can be observed for the largely fed configuration (C); this confirms that the stronger the flow rate, the less perturbed will be the flow. It can be noticed that in the case of jets, similar profiles were observed by Wyganski and Fiedler (1969), who reported a lower value of about 0.24 for the intensity of turbulence relative to the radial velocity component.

Table 3 Turbulence intensity

Authors	Nature of the flow	I_u
Present study	Interaction: plume-stratified media	0.45
Brahimi (1987)	Pure buoyant plume (heated disk)	0.34
Guillou et al. (1986)	Pure buoyant plume (heated portion of a sphere)	0.4–0.5
George et al. (1977)	Plume arising from a hot jet	0.28
Chua and Antonia (1990)	Weakly heated jet	0.22
Wignanski and Fiedler (1969)	Isothermal jet	0.29

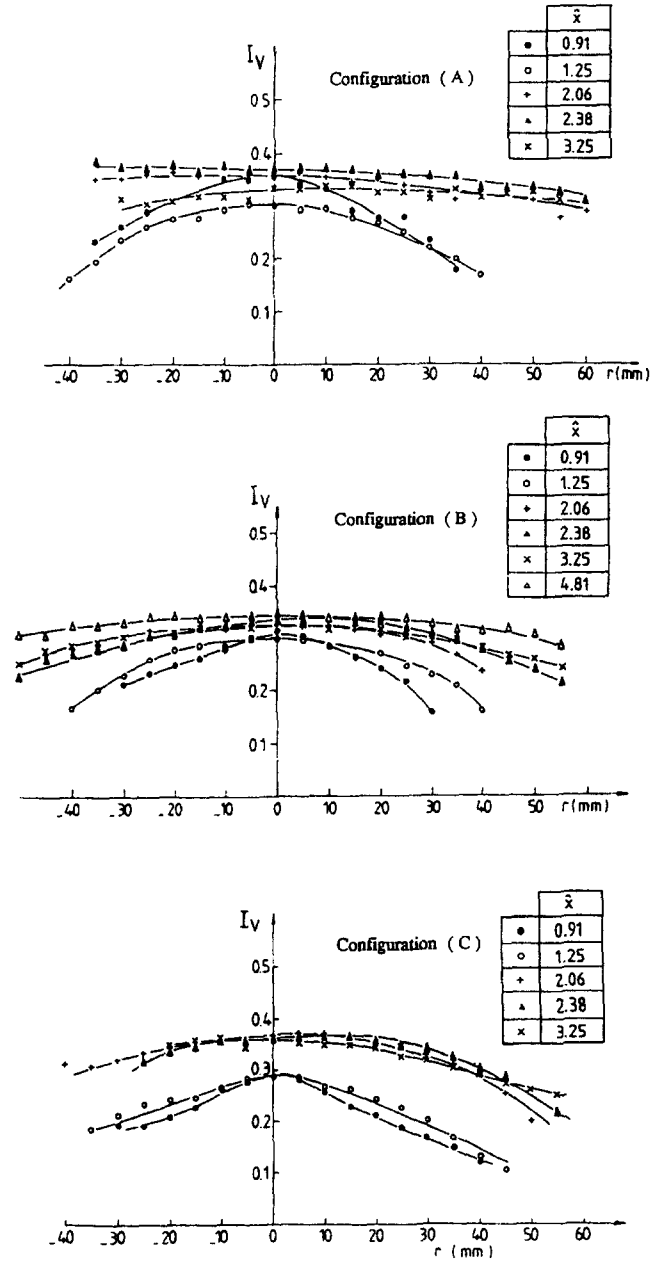

Figure 6 Turbulence intensity of the horizontal velocity

Again, it seems that the increase of the inertia forces results in a decrease of the turbulence. Inside the interaction zone, the intensity profiles become flatter; the flattest profiles can be observed for the weakest flow. For configuration (A) the profiles starting from $\hat{x} = 2.06$ are practically flat, which shows that the interface leads to a homogenization of the turbulence. Inside this zone, in the case of a high flow rate, the impingement on the interface could also be responsible for the increase of I_v.

The distribution of the fluctuations becomes more homogeneous in the neutral zone. I_v is practically constant and averages 0.34 for the three configurations. The turbulence intensity is higher than in the plume area, the difference between these two zones increases with the increase of the flow rate at the source. A definitive separation can be observed for the highest injection value.

To summarize, the turbulence intensity of the radial velocity is quite strong and of the same order of magnitude as the vertical intensity of turbulence I_u. The flow appears to be very disturbed, thus making more difficulties of the measurement of the horizontal velocity component. On the other hand, such perturbations could introduce a certain asymmetry in the $\bar{v}$-profiles.

In the literature, few of these measurements are reported. Nevertheless, the investigations of Guillou (1984), Brahimi (1987) and Brahimi et al. (1989), who found a weaker turbulence intensity I_v almost equal to 0.16 for pure plumes must be mentioned. According to these authors, the strong turbulence intensities are situated farther from the source, as opposed to our case, where they appear near the flow origin due to the strong density difference between the flow and the ambient.

Turbulence kinetic energy. The axial profile of the turbulence kinetic energy $\bar{k} \approx (1/2)(\overline{u'^2} + 2\overline{v'^2})$ differs strongly from one configuration to the other (Figure 7a). It is assumed that the rms values of v' and w' are of the same order and that the relative errors on them are of the order of $\Delta\bar{u}/\bar{u}$ and $\Delta\bar{v}/\bar{v}$, respectively. It is found that $\Delta\bar{k}/\bar{k}$ is 11%.

For configuration (C), $\bar{k}$ increases in the plume zone and is greater than that of configuration (A) by a factor three. The substantial increase of $\bar{k}$ encountered especially with configuration (C) arises from the deep ambient air penetration created by a significant density difference. This increase of $\bar{k}$ is located at the interface for configuration (C). The increase is enhanced by the strong impingement of the flow at the interface. Above the interface, $\bar{k}$ decreases for all the configurations investigated in the neutral medium.

The intensity of the turbulence kinetic energy $\bar{k}/\bar{u}_c^2$ shown in Figure 7b, decreases very abruptly in the plume zone, denoting that the increase of $\bar{k}$, remarked particularly in configuration (C), is occulted by a significant increase of the axial velocity. From the interaction zone, $\bar{k}/\bar{u}_c^2$ is practically constant for the three configurations at an average value of about 0.23.

The radial change for $\bar{k}$ for configuration (B) shows clearly that the maximum of the turbulence kinetic energy is located at the core axis of the plume (Figure 8). The same can be observed for the two other configurations, with an increase of the axial velocity. From the interaction zone, $\bar{k}/\bar{u}_c^2$ is practically constant for the three configurations at an average value of about 0.23.

The radial change of $\bar{k}$ for configuration (B) shows clearly that the maximum of the turbulence kinetic energy is located at the core axis of the plume (Figure 8). The same can be observed for the two other configurations.

In the interaction zone, the profiles become flatter; the degree of flatness increases when the mass flow rate at the source decreases. The flattest profiles are encountered in the case of configuration (A). In the neutral zone, the turbulence energy tends to be weaker and more uniform.

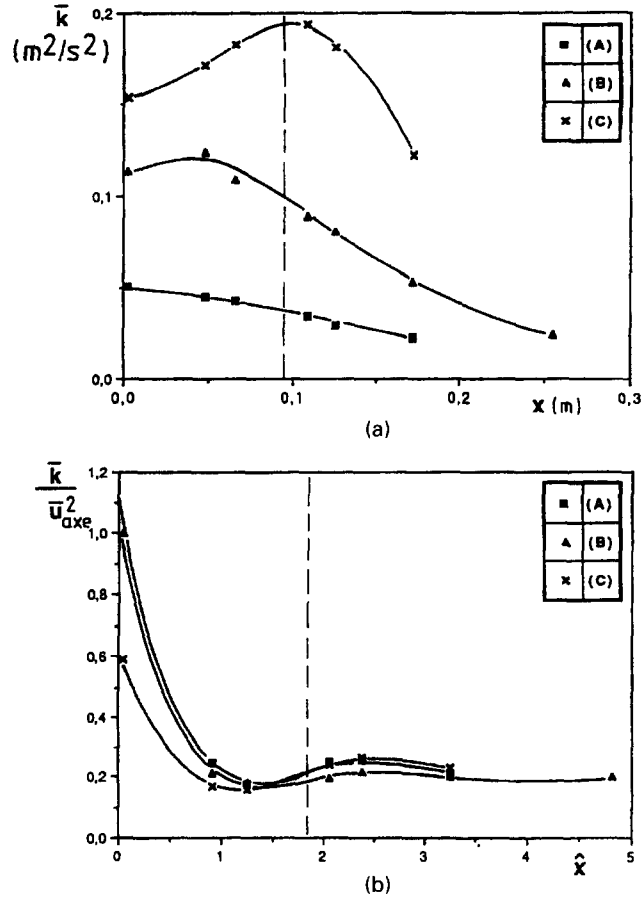

Figure 7 (a) Axial dimensional and (b) dimensionless change of the turbulence kinetic energy.

Conclusion

For the three experimental configurations investigated, we conclude that, in the plume zone, the buoyancy forces play an essential role in the development of the flow. Inside this zone, the form and the amplitude of the dynamic profiles evolve significantly. The zones of strong air entrainment move away from the core of the flow when the height increases.

The turbulence intensity of the horizontal velocity I_v is strong and of the same order as the turbulence intensity of the vertical velocity I_u. The interaction with the stratified media is marked essentially by a decrease of the turbulence rate, by a change of the direction of the radial velocity close to the axis, and by a modification of the geometry of the flow which becomes flatter. For all the configurations investigated, a decrease of the kinetic turbulence energy can be noticed through the neutral medium. In this zone, the flow becomes a pure jet which develops only by the inertia forces. Such correlated information on the fine turbulent structure of the flow, are of interest for a suitable closure of numerical model.

References

Brahimi, M. 1987. Structure turbulente des panaches thermiques—Interaction. Thèse de Docteur de l'Université de Poitiers, Poitiers, France

Brahimi, M., Dehmani, L. and Doan Kim-Son. 1989. Structure turbulente de l'écoulement d'interaction de deux panaches thermiques, *Int. J. Heat Mass Transfer*, **32**, 1551–1559

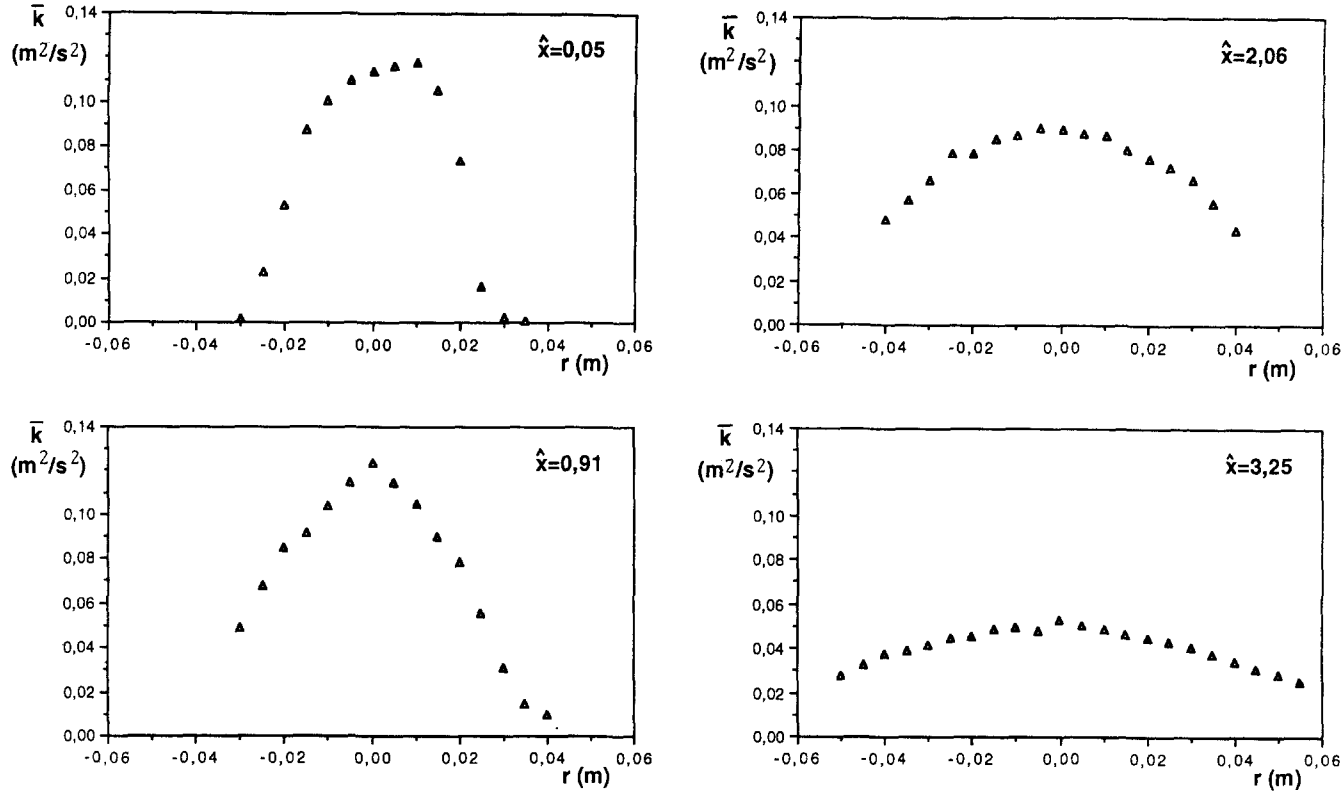

Figure 8 Radial distribution of the turbulence kinetic energy: Configuration (B)

Chen, C. J. and Rodi, W. 1980. Vertical turbulent buoyant jets. In *A Review of Experimental Data, HMT, The Scientific Application of Heat and Mass Transfer*, vol. 4, ch. 6, pp. 59–65, Pergamon Press, London

Chua, L. P. and Antonia, R. A. 1990. Turbulent Prandtl number in a circular jet. *Int. J. Heat Mass Transfer*, **33**, 331–339

Cooper, L. Y. 1983. A buoyant source in the lower of two, homogeneous, stably stratified layers—A problem of fire in an enclosure. National Bureau of Standards, U.S. Department of Commerce, Washington, DC, NBSIR 83-2789

Evans, D. D. 1983. Calculating fire plume characteristics in a two-layer environment. National Bureau of Standards, U.S. Department of Commerce, Washington, DC, NBSIR 83-2670

Gebhart, B., Hilder, D. S. and Kelleher, M. 1984. *The Diffusion of Turbulent Buoyant Jets*. Academic Press, Orlando, FL, 31–57

Gengembre, E. 1983. Contribution à l'étude des flammes de diffusion turbulentes à bas nombre de FROUDE. Thèse de Docteur Ingénieur, Université de Poitiers, Poitiers, France

George, W. K., Alpert, R. L. and Tamanini, F. 1977. Turbulence measurements in an axisymmetric buoyant plume. *Int. J. Heat Mass Transfer*, **20**, 1145–1154

Guillou, B. 1984. Etude numérique et expérimentale de la structure turbulente d'un panache pur à symétrie axiale. Thèse de Docteur Ingénieur, Université de Poitiers, Poitiers, France

Guillou, B., Brahimi, M. and Doan Kim-Son. 1986. Structure turbulente d'un panache thermique. Aspect dynamique, *J. Mécanique Théorique et Appliquée*, **5**, 371–401

Jaluria, Y. and Himasekhar, K. 1983. Buoyance-induced two-dimensional vertical flows in a thermally stratified environment. *Computers and Fluids*, **11**, 39–49

Kapoor, K. and Jaluria, Y. 1993. Penetrative convection of a plane turbulent wall jet in a two-layer thermally stable environment: A problem in enclosure fires. *Int. J. Heat Mass Transfer*, **36**, 155–167

Srinivasan, J. and Angirasa, D. 1990. Laminar axisymmetric multicomponent buoyant plumes in a thermally stratified medium. *Int. J. Heat Mass Transfer*, **33**, 1751–1757

Vachon, M. and Champion, M. 1986. Integral model of a flame with large buoyancy effects. *Combustion and Flame*, **63**, 269–278

Wyganski, I. and Fiedler, H. 1969. Some measurements in the self-preserving jet. *J. Fluid Mech.*, **38**, 577–612